Mapping cerebrovascular reactivity using breath-hold and fMRI: Application to migraine patients and hormonal controls

Ana Beatriz Brissos Raposo - ana.b.raposo@tecnico.ulisboa.pt

Instituto Superior Técnico, Lisbon, Portugal

December 2021

Abstract

Migraine is a disabling disease that is highly complex and incompletely understood. Cerebrovascular reactivity (CVR) measurements have the potential to detect cerebrovascular impairment and have been shown to be altered in migraine. Given this, the objective of this work was to to clarify neurovascular mechanisms by investigating CVR changes during pain (ictal) and pain-free (interictal) phases in migraine. Patients with menstrually-related migraine were selected in order to facilitate the study of the two phases. To control for the effects of hormonal variations associated with the menstrual cycle, healthy controls were studied in the premenstrual and midcycle phases. Blood-oxygenation Level Dependent-functional Magnetic Resonance Imaging (BOLD-fMRI) data were acquired during a breath-holding (BH) task and analysed using 3 methods (one $PETCO_2$-based and two paradigm-based) to obtain maps characterizing CVR. In the control group, increased CVR and reduced delays were detected in the premenstrual vs midcycle session (not significant). Additionally, the group delay maps showed alterations in the posterior area that included the occipital lobe region and the CVR in the occipital lobe was increased in the premenstrual vs the midcycle sessions (not significant). This suggests that alterations in the occipital region in migraineurs during the ictal phase described in previous studies are associated with alterations related to the menstrual cycle and not with the migraine. These findings contribute with new evidence to the limited literature, being the first work investigating CVR in both migraineurs and hormonal controls in a longitudinal approach.

Keywords: Cerebrovascular Reactivity; Functional Magnetic Resonance Imaging; Breath-holding; Menstrually-related Migraine; Hormonal Controls.

1. Introduction

1.1. Motivation

Migraine is one of the most prevalent and disabling diseases on a global scale [1–6], predominantly affecting young women in their most productive life years [3, 4, 7, 8]. Moreover, it is a cyclic disorder composed of headache attacks with other associated symptoms (ictal) and attack-free (interictal) periods that is thought to result from a combination of genetic, environmental and other factors, which makes it highly complex and incompletely understood [7, 9–11]. Currently, there are no biomarkers used in the clinical practice to help the diagnosis process or effective treatment to end or prevent attacks [7, 10, 11].

Migraine has been associated with cerebrovascular [12–15] and cardiovascular diseases [16–18]. In recent years, it has been suggested that this vasculopathy may be related with a dysfunction in the cerebral endothelium [17]. Furthermore, in the case of menstrual and menstrually-related migraine, perimenstrual attacks seem to be triggered by the estradiol decrease prior to menstruation [19–23]. Estradiol plays an important role in the regulation of the vascular endothelium [22], which means that the possible impairment of the cerebrovascular endothelium and vasculopathy in migraine may be intensified near menstruation [24]. Therefore, it seems important to study and take into account the effect of menstrual cycle hormonal alterations when assessing cerebrovascular function in menstrual migraine. However, there are few studies evaluating cerebrovascular changes through the menstrual cycle and the menstrual migraine cycle.

Cerebrovascular reactivity (CVR) measurements have great potential as a way to detect the suspected brain vascular endothelium dysfunction. There are only few studies assessing CVR in migraine and this was commonly done using Transcranial Doppler (TCD). Recently, Blood-oxygenation Level Dependent-functional Magnetic Resonance Imaging (BOLD-fMRI) has been shown to be a more promising technique to measure CVR than TCD. However, there were only two studies assessing CVR in migraine using BOLD-fMRI [25, 26]. Additionally, most studies investigated CVR in a case-control approach, assessing it in the interictal phase of migraine. Being migraine a cyclic disorder, greater potential could be achieved by performing a longitudinal study, studying patients in both phases. This was done in a previous dissertation analysing data from a study that made use of BOLD-fMRI and a breath-holding (BH) task. It was shown that there is increased CVR in the occipital area of migraineurs in the ictal phase, when compared to the interictal phase [26]. However, this study did not include controls. More significant results should be achieved by taking into account the cerebrovascular alterations through the menstrual cycle. Additionally, although a BH task has been done, the partial pressure of end-tidal carbon dioxide ($PetCO_2$), a surrogate of the partial pressure of arterial CO_2 ($PaCO_2$), was not recorded, which could take into account the variations in task performance and normalize CVR measurements [27–30].

1.2. Migraine

Migraine affects approximately 14% of the worldwide population and is the second in years lived with disability [1–5]. Migraine predominantly affects women, following a 3:1 ratio [8]. Specifically, it is more prevalent among young and middle-aged women between ages 15 and 49, which usually correspond to their most productive life years. In this group, migraine assumes the first place in years lived with disability [3, 4, 7].

Migraine is a cyclic disorder as it is composed of an ictal state with unilateral throbbing headache and other associated symptoms, alternated with an attack-free interictal state. In the ictal state, 4 phases of the attack can be defined: the premonitory, aura, headache and postdrome [8, 11, 31]. The headache phase is the most notorious phase in migraine episodes and all the phases can appear in the mentioned sequential order or overlap [5, 8].

The pathophysiology of migraine has shown to be highly complex and still incompletely understood. Nevertheless, the consensus nowadays points towards a neurovascular hypothesis [5, 7, 8, 11, 16]. In fact, the association between migraine and cerebrovascular and cardiovascular diseases supports the idea of a dysfunctional cerebral endothelium in migraine [13–18].

Throughout the reproductive years, menstruation is one of the events that shows higher association with migraine attacks [32]. Menstrual migraine (MM) is the migraine that occurs between 2 days before and 3 days after menstruation in at least two out of three menstrual cycles, with no attacks at any other time of the menstrual cycle. This is only reported by 10% to 20% of female migraineurs. In turn, menstrually-related migraine (MRM) is the one occurring in the previously mentioned conditions and additionally at other times of the menstrual cycle and this is prevalent in more than half of female migraineurs [20, 32–34]. Perimenstrual attacks are usually longer, more incapacitating, recurrent, painful and less responsive to treatment compared to attacks at other times of the cycle or to non-menstrual migraineurs' attacks [6, 20, 21, 23, 32]. In patients suffering from menstrual or menstrually-related migraine, perimenstrual attacks seem to be triggered by the premenstrual decrease of the ovarian hormone estradiol (E2). E2, in turn, is thought to be involved in the regulation of the vascular endothelium and is associated with reduced stroke risk and favorable stroke outcomes. This supports the theory of a dysfuntional cerebral endothelium in migraine and suggests that this impairment is intensified near menstruation. Furthermore, it seems important to study and take into account the effects of the hormonal alterations through the menstrual cycle when studying cerebrovascular function in migraine.

1.3. Cerebrovascular reactivity

Cerebrovascular reactivity (CVR) is an intrinsic regulatory brain mechanism that reflects the capability of its vessels to alter their calibre in response to a vasoactive stimulus, whether by dilating or constricting, with the objective to increase or decrease cerebral blood flow (CBF). If CVR is impaired, then CBF cannot increase when brain activity increases. Thus, CVR can be thought of as an indicator of brain's vascular health. CVR measurements have the potential to detect cerebrovascular impairment and have been shown to be altered in migraine.

To determine CVR, the CBF changes are measured simultaneously to the application of a vasoactive stimulus. BOLD-fMRI has shown to be an appropriate measurement technique, enabling non-invasive whole-brain scannings with high spatial resolution. As concerns the vasoactive stimulus, the BH task seems to be appropriate it has been shown to be non-invasive and simple in terms of execution and experimental setup.

1.4. State of the art

A literature review was handled regarding CVR in migraine, menstrual cycle and menstrual and menstrually-related migraine. Most studies used BH as vasoactive stimulus and TCD as CBF measurement technique. The BOLD-fMRI technique has been shown to be a more promising technique to measure CVR than TCD, but only 2 studies have used fMRI to study CVR in migraine [25, 26].

Most studies investigated CVR in migraine in a case-control approach, assessing it in the interictal phase of migraine and comparing it with healthy controls. From these, CVR was suggested to be impaired in the posterior circulation of migraineurs [12,35,36]. Being migraine a cyclic disorder, greater potential could be achieved by performing a longitudinal study. This was done in some studies, in which the CVR in the ictal phase showed to be lower than in the interictal phase of migraine [37–40]. Furthermore, in a study done in the same lab as this work, LaSEEB of ISR-Lisbon, Cotrim et al. [26] analysed BH BOLD-fMRI data and showed increased CVR in the occipital area of migraineurs in the ictal phase, when compared to the interictal phase. However, this study did not include controls.

There were only 2 studies evaluating cerebrovascular changes throughout the natural menstrual cycle of healthy women. One [41] measured CBF during the early follicular, late follicular and late luteal phases and suggested that the CVR of the brain parts supplied by the right internal carotid artery (ICA) varied significantly during the menstrual cycle and that these variations seemed to be associated with the levels of the ovarian hormones estradiol and progesterone. The other one [22] assessed CBF during the early and late follicular phases and no difference in CVR was verified.

Finally, no studies investigated CVR in menstrually-related migraine and only 2 studies investigated CVR in menstrual migraine without including hormonal controls. One scanned patients without accounting for the migraine cycle phase [34]. CVR of the middle cerebral arteries (MCA) was found to be reduced during the menstruation when compared to the period after menstruation and CVR of the MCA and posterior cerebral arteries (PCA) was detected to be reduced when compared to controls. The most recent one studied migraine interictal phase [20] and no differences in the CVR were found.

As a way to overcome these bottlenecks, we propose to investigate the CVR changes through the analysis of BH BOLD-fMRI data from menstrual or menstrually-

related migraine patiens in ictal and interictal phases; and hormonal controls in premenstrual and midcycle phases.

2. Material and methods

2.1. Breath-holding task

An illustration of the BH-task paradigm is illustrated in figure 1. It comprised a 30s initial baseline of externally-paced breathing and four 58.5s cycles (resulting in a total duration of 269s, approximately 4.5 minutes taking into account a 5s fixation cross). Each cycle consisted of a 15s end-expiration BH followed by a 1.5s exhalation, a subsequent 12s recovery period with self-paced natural breathing and finally a return to 30s baseline of externally-paced breathing. Regarding the baseline periods (both the initial baseline and each trial's baseline), these were externally-paced at a breathing period that was the most similar to the subject's spontaneous breathing period (to avoid hypocapnia). These parameters were according to the literature and tests. Tests were performed at LaSEEB with 7 female gender adults aged from 20 to 55 years that were professors, investigators or students. Additionally, a pilot study was performed at Hospital da Luz (Lisbon, Portugal) with one of these volunteers to test the BH task along with the fMRI scan. During these tests, after the task was performed it was asked if the volunteer had found it hard to perform in general, e.g. had felt tired in general, had found the task too long, had found hard to sustain the breath during the BH period, to exhale after the BH, or to breath according to the instructions during the baseline periods.

An illustration of the experimental setup for recording of the PetCO_2 during the BH BOLD-fMRI acquisition is presented in figure 2. The written task instructions were given to the subjects visually by being projected from a computer (the Presentation computer) where they had been programmed in the Neurobehavioral Systems Presentation software (`https://www.neurobs.com/`) to the googles on the head radiofrequency coil. Measurement of CO_2 levels of expired air data was carried out using the Medlab CAP10 capnograph (`https://www.medlab.eu/english/products/capnographs/cap10`) and a tubing system (composed of a nasal cannula and sampling lines). The Presentation codes relative to the instructions being displayed to the subject and the CO_2 data being acquired in the capnograph and passing through the analog to digital converter Arduino UNO (`https://store.arduino.cc/products/arduino-uno-rev3/`) were both recorded in a computer (the recording computer).

2.2. Participants and data acquisition

A longitudinal study was conducted in the Imagiology Center of Hospital da Luz (Lisbon, Portugal) in the period from May to October 2021. The cases comprised 3 female patients (mean age = 35.33$\pm$9.29 years old) from the Hospital da Luz outpatient clinic with a diagnosis of menstrually-related episodic migraine without aura and otherwise healthy. The control group was composed of 6 healthy women (mean age = 25.50$\pm$3.08 years) recruited among social media, migraine groups, academic groups and internal mailing lists, who had no history of migraine or headaches and had regular menstrual cycles. Both cases and controls could be using hormonal contraception during the study provided that they still had menstruation and were able to track their menstrual cycle.

Each patient was scanned in the ictal (headache) and interictal phases of migraine. The ictal phase scanning session was performed during an attack indicated by the patient. Scanning of controls happened in in the premenstrual and in the midcycle phase of the menstrual cycle. The premenstrual phase was considered to be 1 to 4 days before menstruation onset and the midcycle phase 1 to 4 days after ovulation (ovulation being forecasted by natural menstrual cycle monitoring through the calendar method and sometimes basal temperature measurement and in day 14 of the menstrual cycle for the participants taking the pill). However, in some cases, it was not possibly to acquire both sessions of a volunteer due to the inherent unpredictability of the migraine and to hospital logistics issues, the latter having been exacerbated by the pandemic. Therefore, only 2/3 patients and 5/6 controls concluded the two sessions within the duration of the work leading up to this dissertation.

Two types of data were acquired for each participant, for each acquisition: brain imaging and expired CO_2 data.

All images were acquired with a 3T Siemens MAGNETOM Vida MRI scanner using a 64-channel receive radiofrequency coil. Structural T1-weighted images were collected using a MPRAGE sequence (1 mm isotropic resolution). T2*-weighted 2D GE-EPI was acquired (SMS = 3, GRAPPA = 2, TR=1260ms, TE=30ms, 213 volumes, effective EPI echo spacing 0.31ms and 2.2mm isotropic resolution). Fieldmap images were collected using GE-EPI (TE1/TE2 = 4.92/7.38 ms and otherwise similar geometry to the functional images).

During the BOLD imaging of the BH task, the expired CO_2 was simultaneously acquired using the experimental setup (both described in section 2.1). To assure that the BH task was well executed and that the CO_2 was properly measured inside the scanner, the participants' preparation started outside the scanner. The task was explained to the participants, enhancing the importance of breathing through nose and not to inspire during the BH. After this, each participant's spontaneous breathing period was measured and calculated and, according to it, one or more practice runs were performed with live visualization of the expired CO_2 signal. Afterwards, the participant was directed to the scanner room.

2.3. CO_2 data processing and analysis

Processing and analysis of the CO_2 signal acquired were conducted using the MATLAB software (`https://www.mathworks.com/products/matlab.html`).

First of all, the custom peak detection algorithm was applied to the acquired breathing period CO_2 data in order to detect the end-tidal peaks - level of CO_2 released at the end of exhalations. The output was manually checked for every dataset to ensure that each end-tidal peak was detected and to remove incorrectly identified ones

Each CO_2 recording was longer at least 30s before and after each fMRI acquisition. The time period af-

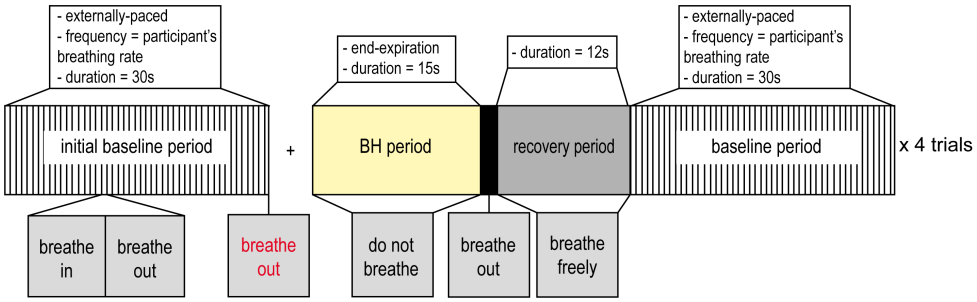

Figure 1: Schematic illustration of the breath-holding task paradigm.

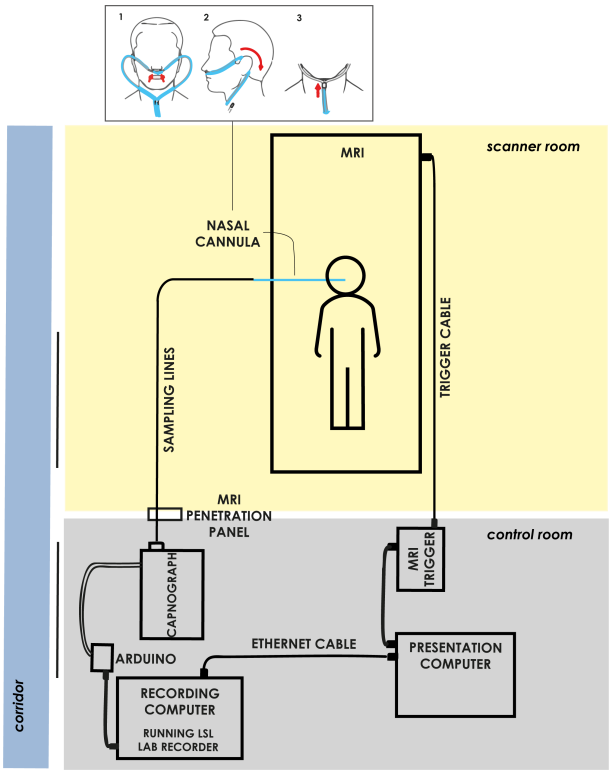

Figure 2: Schematic illustration of the breath-holding task experimental setup

ter makes it possible to correct for the recording delay between CO_2 exhalation inside the scanner and CO_2 recording outside the scanner. In fact, a negative time shift was applied to the CO_2 data in order to align their post-BH exhalations to the respective markers from Presentation. On the other hand, the time period added before was due the hemodynamic delay between the CO_2 pressure change in the blood and the fMRI signal change caused by the vascular transit delays and vasodilatory dynamics, which will be used in further data processing.

The CO_2 data corrected for the recording delay was similarly processed to the breathing periods in order to detect the end-tidal CO_2 peaks. From these, the $PetCO_2$ trace was produced by using a piecewise cubic interpolation between the end-tidal peaks to the capnograph sampling interval. For each subject and session, the mean baseline $PetCO_2$ and the mean $\Delta PetCO_2$ were calculated. Finally, a $PetCO_2$ regressor was created by convolving the $PetCO_2$ trace with the canonical hemodynamic response function (HRF) [27, 28, 42].

2.4. BOLD-fMRI data processing and analysis

Processing and analysis of the BOLD-fMRI was conducted using both the FMRIB Software Library (FSL, `https://fsl.fmrib.ox.ac.uk/fsl/fslwiki/`) and the MATLAB software.

It is crucial to perform some preprocessing to the fMRI data to remove unwanted artifacts that may complicate its interpretation. Moreover, the performance of BH tasks typically adds task-correlated motion to the data [43]. Therefore, the preprocessing steps done in this work were: (i) distortion correction (using FUGUE); (ii) motion correction (using MCFLIRT); (iii) spatial smoothing (using SUSAN); (iv) high-pass temporal filtering (using FEAT); (v) nuisance regression of motion parameters (using MCFLIRT); and (vi) nuisance regression of motion outliers (using fsl_motion_outliers). Nuisance regressors of motion parameters and motion outliers were introduced together with the regressors of interest during the BH BOLD-fMRI analysis that will be further discussed in section 2.5.

Registration of the subjects' functional images to the structural space (using FLIRT BBR) and normalization to the standard space (using FNIRT) were also performed. This is important to align the images of different sessions and subjects with each other so that posterior analysis steps are valid. Lastly, the two transformations were combined, defining a single transformation from the functional to the standard space.

When looking for CVR in migraine, an initial approach may consist of a whole-brain voxelwise analysis. However, it may also be relevant to focus the analysis into specific brain regions with the objective of identifying impaired areas. Bearing this in mind, three categories of regions-of-interest (ROIs) were defined: cortical lobes (frontal, temporal, parietal and occipital), arterial flow territories (internal carotid arteries, ICA, and vertebrobasilar arteries, VBA) and subcortical structures (brainstem, thalamus, pallidum, putamen, hippocampus and caudate). For this, brain masks of these regions were created. They were defined within gray matter (GM) as this is a much more vascularized area [44] and exhibits greater BOLD signal change when compared to the white matter (WM) [30, 45, 46].

2.5. Breath-holding BOLD-fMRI data analysis

Concerning the BH BOLD-fMRI data analysis, this is usually performed using the General Linear Model (GLM) in FEAT (`https://fsl.fmrib.ox.ac.uk/fsl/fslwiki/FEAT`). Furthermore, CVR characterization must be performed on a voxelwise basis, since the

BOLD hemodynamic response may exhibit different temporal dynamics in different brain regions that in turn affect CVR estimation. Taking this into consideration, the analysis was performed using a $PetCO_2$-based method (the iteratively shifted $PetCO_2$ regressors GLM) and two paradigm-based methods (the iteratively shifted block-design regressors GLM and the sine-cosine GLM).

$PetCO_2$-based models account for variability in task performance and in the resulting $PaCO_2$ levels, whether across subjects, sessions or even trials. The iteratively shifted $PetCO_2$ regressors GLM started by performing an initial global gross alignment by maximizing the cross-correlation between the mean global GM BOLD time-course linearly up-sampled to the capnograph sampling frequency and the $PetCO_2$ regressor that overlapped the fMRI acquisition. From the resulting delay - the bulk shift - 61 shifted $PetCO_2$ regressors relatively to this value, up to a maximum shift of $\pm$9s, with an increment of 0.3s [43, 47] and downsampled to TR were created. For each of these regressors, a GLM was constructed (including its temporal derivative). Motion parameters and motion outliers were also included in the model as regressors of no interest. CVR in percent signal change (PSC) was calculated for each one of the 61 obtained GLMs, following the formula:

$$\text{CVR in PSC } (\%) = \frac{PE1 * 100}{meanfunc} \quad (1)$$

where PE1 is the parameter estimate image that informs about how strongly the $PetCO_2$ regressor fits the data at each voxel and *mean func* is the mean data over time at each voxel. In this case, as the regressors given to the model were not normalized by FEAT, the PE1 maps are per change in expired CO_2 (mm Hg) and consequently, vascular reactivity was defined as CO_2-related BOLD percent signal change/mm Hg change in CO_2 (%/mm Hg). The 61 PSC maps were then merged and on a voxelwise basis, the delay at which the CVR was highest in that voxel (which corresponds to the highest PE1 value and thus to the shifted regressor that better fits the data) was chosen as the optimal delay, resulting in a map of delays (s). The same was done to obtain a map of CVR (%/mm Hg). This was done for all the sessions in which a valid CO_2 signal was acquired.

The models used in paradigm-based analysis are a representation of what is expected to be observed in the data: changes in BOLD hemodynamic response in response to a certain stimulus. A perfect performance is assumed, as well as similar BH effects on the $PaCO_2$ within and between subjects. Thus, the regressors given to the models were derived from the timings of BH-task paradigm presented in each scanning session.

Similarly to iteratively shifted $PetCO_2$ regressors GLM, the iteratively shifted block regressors GLM starts by maximizing the cross-correlation between the mean global GM BOLD time-course linearly up-sampled to a sampling interval of 0.02s (having this value been chosen in order to maintain a good temporal resolution) and the block regressor - a square box function with an amplitude of 1 during the four BH periods and 0 during the baseline and recovery periods, convolved with the canonical HRF - from which results a bulk shift value. Once more, 61 shifted block regressors (downsampled to TR) were created, from which 61 models were constructed (including its TD, motion parameters and motion outliers). To create the CVR and the corresponding delay maps, the same process that had been done in the iteratively shifted $PetCO_2$ regressors GLM method was done. However, the block regressor was automatically normalized by FEAT and thus, the 61 resulting CVR maps and the final CVR maps were presented in PSC.

The other paradigm-based method used was the sine-cosine GLM consisting of a sine-cosine pair at the BH task period (58.5s) and its first two harmonics based on previous work optimising the number of harmonics [48]. Motion parameters and motion outliers were also included in the model as regressors of no interest. Furthermore, as the task cycles only begin after 35s (5s of fixation cross plus 30s of initial baseline) of task performance, this model has an initial skip with this duration (as it was concluded that this improved model fitting in comparison to the sine-cosine model beginning at time t=0s). As a single GLM resulted from this analysis and it already accounts for voxelwise variations with its inherent phase flexibility, voxelwise CVR and delay maps were constructed differently from the two previous methods. CVR (in BOLD PSC, %) was calculated as the amplitude of the model's maximum relative to the average initial baseline signal multiplied by 100 and the delay time-to-peak (TTP) as the time of the model's maximum relative to the beginning of the BH (in seconds). To achieve this, the sine and cosine waves and their first and second harmonics and respective parameter estimates values were imported into MATLAB and used in order to create an averaged model at each voxel and from it compute the CVR and TTP.

In order to be able to compare the CVR maps resulting from the paradigm-based methods (in %) with the ones resulting from the $PetCO_2$-based method (in %/mm Hg), the latter were multiplied by the $\triangle PetCO_2$ (calculated by subtracting, for each task cycle, the value of the post-BH $PetCO_2$ by the mean baseline $PetCO_2$ of the previous baseline period and averaging across the four cycles). On the other hand, as CVR in %/mm Hg accounts for variability and allows to quantitatively compare CVR between sessions and individuals, CVR maps obtained through the paradigm-based methods were divided by the corresponding $\triangle PetCO_2$ in order to obtain normalized CVR measures (%/mm Hg) and be able to compare them with the measures resulting from the $PetCO_2$-based model.

Firstly, CVR characterization was executed across voxels in the whole-brain GM for each subject, session and analysis method. On a second phase, CVR characterization for the ROIs corresponding to cortical lobes, arterial territories and subcortical structures within GM was developed (whose masks' construction was described in 2.4).

3. Results & discussion

Both CO_2 and BOLD-fMRI data acquired during a BH task from 3 migraine patients and 6 hormonal controls was processed and analyzed using three different methods. This resulted in CVR and delay maps. The analysis

of these maps enabled to compare the different analysis methods. A group analysis was also performed that allowed for the detection of CVR differences between the different phases, methods and ROIs, but only for controls due to the reduced number of patients.

3.1. $PetCO_2$, motion and cross-correlation analysis

All subjects successfully completed the respiratory protocol with no major difficulties reported, verified by the increase in the mean GM BOLD-fMRI time course in the periods after the BH. However, datasets C1-S2, P1-S1 and P3-S1 (where C represents controls, P patients, S1 the premenstrual/ictal session and S2 the midcycle/interictal session, performed in a random order) revealed low quality CO_2 traces. This may have been caused by periods of exhalation through the mouth, impairing the measurement of the $PetCO_2$ (especially the increase after BH). In these cases, the $PetCO_2$ method of CVR analysis was not performed and $PetCO_2$ normalised CVR measurements were not obtained.

A mean $PetCO_2$ baseline of 36.4±4.5 mm Hg across participants was observed, which is in general agreement with other BH CVR studies [42,49,50] and assures that CVR is measured over the linear range of the CBF-CO_2 dose–response curve, avoiding hypocapnic conditions [51]. Furthermore, a mean $\triangle PetCO_2$ of 5.4$\pm$1.9 mm Hg across participants was calculated, which is in general agreement with other similar BH CVR studies [42, 47, 49, 50]. However, one of the four BH trials were excluded for the calculation of the $\triangle PetCO_2$ in acquisitions C1-S1 and P2-S2, due to automatic calibration of the capnograph during that one BH, which interfered with the correct signal acquisition.

The mean absolute displacements averaged across sessions were 0.39$\pm$0.29 mm, while the mean relative displacements across sessions was 0.11$\pm$0.06 mm. The highest values of displacements were verified to be related with task performance.

The delay introduced by the tubing system was of around 10s in all the acquisitions except in C1-S1 and P1-S1, in which the delay was different because the used tubing system was different.

Regarding the bulk shifts obtained by maximizing the cross-correlation between the unshifted $PetCO_2$ regressors and the mean GM BOLD signal time course for each acquisition, this was 5$\pm$1 s on average across subjects, which is according to the range of from 5s to 10s for average delay times found in literature [42, 52]. As concerns the bulk shift corresponding to the block regressor calculated following the same procedure, the average across subjects was 10$\pm$2 s. This was expected since the block model is created using the timings of the presentation of the stimuli through visual instructions and the $PetCO_2$ changes occur as a consequence of the performance of these instructions, that naturally happens afterwards. Nevertheless, besides the acquisitions with low quality $PetCO_2$, the bulk shifts for both the $PetCO_2$ and the block regressors were also not calculated for the datasets C4-S2 and P3-S2 due to logistics' issues during the acquisitions that impeded the synchronous presentation of the stimuli with the fMRI scanning, thus interfering with the hemodynamic delay estimation. In these cases, the shifted regressors were calculated from the other acquisitions' mean bulk shift.

Cross-correlation analysis between the mean sine-cosine model time-course and the mean GM BOLD-fMRI signal time course was also performed for each session. From this, it could be seen that the sine-cosine model did not present a good fit of the mean GM time course.

3.2. Cerebrovascular reactivity and delay maps

Regarding the CVR and delay maps, average maps across controls are shown in figure 3, respectively. Maps presented the expected contrast between GM and WM: GM presented increased CVR values and decreased delay values when compared to the WM. These results were not surprising since GM is a highly vascularized area and presents a large signal change in most CVR studies [30, 44, 45, 48]. Due to these observations, further CVR characterization focused on the GM. In addition, for the $PetCO_2$ and block methods, the posterior area of the brain presented increased delays when compared to the anterior one, which is according to literature [28, 43, 48]. On the other hand, the sine-cosine method did not present this delay pattern and resulted in a noisier map.

3.3. Whole-brain analysis

3.3.1 Subject-level analysis

The number of voxels with detected CVR (CVR in $\%$ ¿ 0.3) (in $\%$) and the median CVR (in $\%$ $\%$/mm Hg) and delay (in s) across brain in GM were calculated for each subject, session and voxelwise analysis method ($PetCO_2$, block and sine-cosine), such as the group mean for controls and patients for each method.

The iteratively shifted block-design regressors GLM method showed to be the most effective of the 3 methods in modelling BH BOLD-fMRI data as, besides producing the highest percentage of voxels with detected CVR, resulted in the highest CVR amplitude estimates.

As regards the $PetCO_2$ model, this produced percentages of voxels with detected CVR and CVR amplitude estimates higher than the sine-cosine model, which is according to Murphy et al. [42], that concluded that the $PetCO_2$ model leads to a better model fit the sine–cosine, but not in all brain regions. However, it produced lower estimates than the block model. This was not expected since the $PetCO_2$-based models account for variability across and within subjects [29]. This result seems to be due to incorrect CO_2 acquisition caused by experimental setup issues, namely to the use of an exclusively nasal cannula that did not get the expired CO_2 from mouth (that seemed to have frequently occurred although subjects were instructed to breath through their noses).

Finally, the second order sine-cosine model produced the lowest percentage of voxels with detected CVR and estimates of CVR. The second order sine-cosine model that was used in this work had shown to explain significantly more variance, produce a greater number of responsive voxels, not underestimate CVR amplitude and show a better test-retest reproducibility than lower order methods [48]. However, this was proven for a BH task

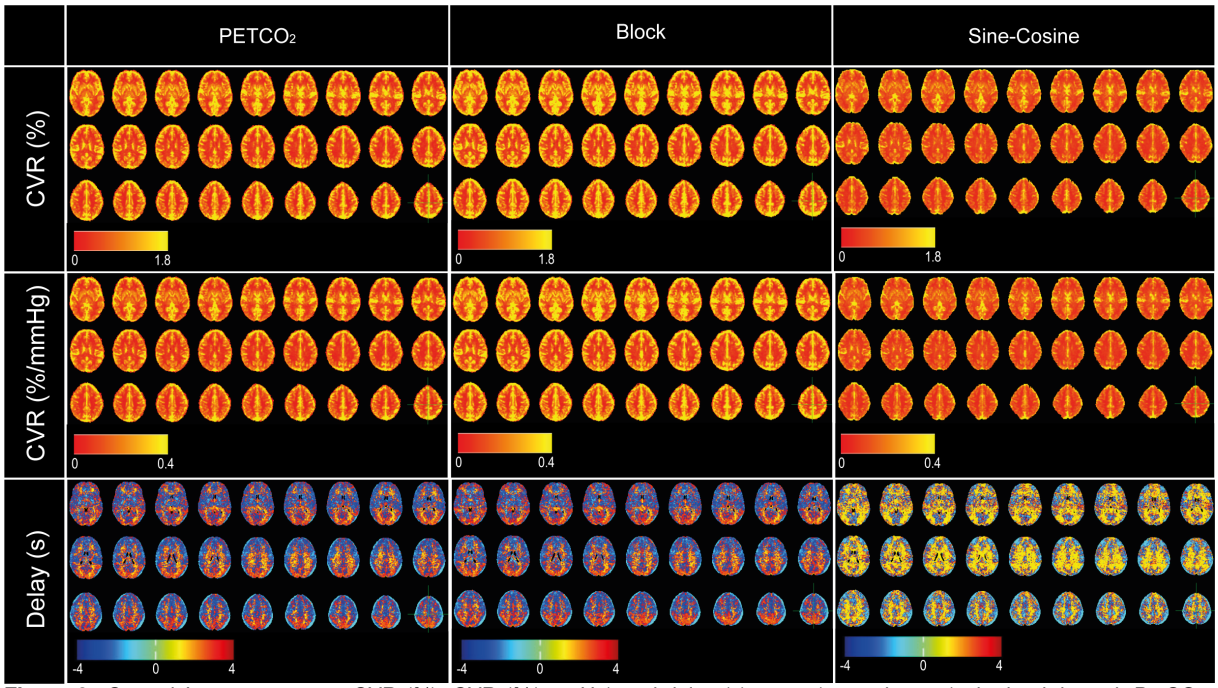

Figure 3: Controls' group average: CVR (%), CVR (%/mm Hg) and delay (s) maps (top to bottom) obtained through $PetCO_2$, block and sine-cosine methods (left to right). The maps are represented in the standard MNI152 space.

with cycles' duration of 75s. In our case, with a task with cycles with 58.5s, the second order model may not be the most appropriate, e.g. the use of more harmonics would perhaps improve the sine-cosine model fitting. The optimal number of harmonics would have to be estimated specifically for our protocol (which was not done in this dissertation).

The normalization of CVR units is crucial as it allows to make an accurate comparison of CVR values between different subjects and sessions. Furthermore, CVR in %/mm Hg had shown to result in more statistically active voxels in task-related analyses at the group level [42]. However, the $\Delta PetCO_2$ used for the normalization is inherently an unstable measure that can easily be skewed by outliers in the $PetCO_2$ trace such as erroneous readings and partial breaths, which may introduce some errors in the results presented in normalized CVR units [42]. Moreover, the normalization may be an oversimplification of the true interrelation between CVR and $PetCO_2$, that also depends on the baseline $PetCO_2$ with nonlinear behavior at maximal vasodilation [28, 50, 51, 53]. Thus, the normalized results obtained may not be completely trustworthy. Nevertheless, the mean median CVR in GM obtained from the $PetCO_2$ and block models, 0.18$\pm$0.04 %/mm Hg and 0.20$\pm$0.10 %/mm Hg, respectively, were according to the literature (reporting a range from 0.15 to 0.40 %/mm Hg). As concerns the sine-cosine model, the median CVR values obtained through its use were lower than the ones reported in literature [27, 29, 43, 47–49, 54].

The delays were generally higher for the block model in comparison to the ones obtained through the $PetCO_2$ model. This was expected due to their origin (timing of the presentation of the stimuli in the block model and timing of the reaction towards the stimuli in the $PetCO_2$ model). Furthermore, they were similar to the previously estimated bulk shifts for the two methods. In respect to the TTP obtained through the sine-cosine model, this metric is intrinsically higher than the previous two. However, TTP has been reported to be 31s for 15s end-expiration BH and between 30s and 40s for 20s end-expiration BH [26, 48]. Therefore, TTP seems to have been underestimated in the present study.

3.3.2 Control group-level analysis

In order to compare controls C2 to C5 (for whom the $PetCO_2$ method of CVR analysis was performed for both the scanning sessions) between the two sessions (premenstrual and midcycle), boxplots representing the distributions of the number of voxels with detected CVR and median CVR and delays for all the analysis methods are presented in figure 4. The distribution of the mean $\Delta PetCO_2$ that is used for the conversion of CVR from % units to %/mm Hg units is also represented.

The block model presents the highest percentage of voxels with detected CVR, the highest estimates of CVR and the least variability across the group, thus seeming once more to be the best model in fitting our BH BOLD-fMRI data. On the other hand, the sine-cosine model seems once more to be the worst.

The number of voxels with detected CVR and the CVR (in %) was found out to be increased in the premenstrual vs midcycle session. However, with CVR normalization, CVR became decreased in the premenstrual session when compared to the midcycle sessions. This can be explained by the increased mean $\Delta PetCO_2$ measures in the premenstrual sessions. The reason for this increase in $\Delta PetCO_2$ is not clear. It is not likely that it is a hormonal effect, so it may have been caused by the inherent

unstable measure of $PetCO_2$, as referred in section 3.1. Finally, lower delays were noticed in the premenstrual sessions (through the $PetCO_2$ and block methods). A repeated measures ANOVA test using the statistics program JASP (`https://jasp-stats.org/`) was performed over the number of voxels with detected CVR, the median CVR values and the median delay values, that revealed a significant main effect of methods in the CVR and delays ($p=0.003$ and $p=0.001$, respectively), but not of the menstrual cycle phases. However, the fact that the differences did not achieve statistical significance may be due to the reduced number of controls.

3.4. Region-specific analysis

Following the whole-brain GM control group analysis (for C2 to C5) of CVR and delay maps, a region-specific voxelwise analysis was performed in these maps in order to assess voxelwise differences of particular brain regions between premenstrual and midcycle sessions. Therefore, the ROIs referred in 2.4 within GM for each subject and session were analysed.

The median of the median CVR (in $\%$) across controls was shown to be increased in the premenstrual session in the the occipital lobe, putamen and caudate. In these regions, the CVR in the premenstrual session was increased when compared to the CVR in the global GM (1.2-1.4$\%$ in these ROIs vs 1.1-1.2$\%$ in the global GM). The visual cortex in the occipital lobe and the putamen had already shown to have increased CVR when compared to the global GM resulting from a BH fMRI [43,49]. In order to further investigate these differences between the premenstrual and midcycle phases, a repeated measures ANOVA test was performed over the within ROI median CVR values, for each ROI, which revealed a significant main effect of ROIs and analysis methods ($p<0.001$), but not of the menstrual cycle phases. Nevertheless, the fact that the differences did not achieve statistical significance may be due to the small sample of controls. As concerns the normalized CVR and the delays among the different ROIs, no differences were verified between the premenstrual and midcycle phases.

4. Conclusions & future work

In the present study, CVR was studied using a BH-task and BOLD-fMRI in a group of patients which was studied during the ictal and interictal phases of migraine and a group of hormonal controls which was studied during the premenstrual and midcycle phases of the menstrual cycle. In the control group, increased CVR (in $\%$) and reduced delays in GM were detected in the premenstrual phase when compared to the midcycle phase, although not significant. In previous studies, the PCA had been reported to be reduced in migraineurs when compared to controls [12, 35, 36]. Furthermore, in a study from Sofia et al. [26], CVR and TTP were found out to be increased in the occipital lobe during the ictal compared with the interictal phase in migraine patients. In the present work, the group delay maps showed alterations in the posterior area that included the occipital lobe region and the CVR of controls in the occipital lobe was increased in the premenstrual vs the midcycle session. This may imply that the alterations in the occipital region in migraineurs during the ictal phase described in previous studies [26] may in fact be associated with (possibly hormonal) alterations related to the menstrual cycle and not characteristic of the migraine disorder (that had been associated with an endothelial dysfunction of the posterior cerebral circulation [26, 35]). This enhances the importance of including appropriate controls in studies, even when following a longitudinal approach.

Three different methods were implemented to analyse CVR: the iteratively shifted $PetCO_2$ regressors GLM, the iteratively shifted block regressors GLM and the sine-cosine GLM methods. The results showed that the iteratively shifted block regressors GLM method was the most effective in modelling the BH BOLD-fMRI data as it produced the highest percentage of voxels with detected CVR and highest CVR amplitude estimates. On the other hand, the relative underestimation of the iteratively shifted $PetCO_2$ regressors GLM methods seems to be due to incorrect CO_2 recording caused by the use of an exclusively nasal cannula that did not account for the CO_2 signal expired through the mouth. Nevertheless, both of these methods produced maps with expected contrast between GM and WM and showed higher delays in the posterior region of the brain, according to the existing literature [28, 30, 43–45, 48]. In turn, the sine-cosine GLM model showed to be the worst in fitting the data, which can be justified by the incorrect number of harmonics. Additionally, the delay maps obtained through this method were the noisiest. As concerns the normalized CVR, this accounts for the variability in the task performance and allows to make a more accurate comparison between different subjects and sessions. However, the $\Delta PetCO_2$ in our case is prone to have misleading values due to experimental setup issues, which may have introduced some errors and alter the results, so they must be dealt with caution.

This dissertation was, as far as we know, the first work investigating CVR in both migraineurs and hormonal controls in a longitudinal approach (studying patients' ictal and interictal phases and controls' premenstrual and midcycle phases). In fact, only two studies have assessed CVR in menstrual migraine and did not include hormonal controls [20, 34]. Additionally, only two studies were found in literature that have evaluated CVR in the menstrual cycle following a longitudinal approach [22, 41]. All these used TCD and not fMRI, lacking spatial resolution. This study also contributes for the scarce information about the BH paradigm design parameters, experimental setup, and analysis methods that can be used to model this type of data.

4.1. Limitations and future work

The BH performed by the subjects in this study was preceded by an expiration and followed by periods of externally-paced breathing according to the subjects' natural breathing rate [27–30, 42]. However, end-inspiration protocols are easier to perform and therefore could lead to better results when dealing with less cooperative patients (in ictal phase). Using computer-paced breathing according to the subjects' breathing rate reduces possible inter- and intra-subjects CBF differences arising from CO_2 variations caused by subjects' ventilation and lung function [28, 30]. However, it may induce

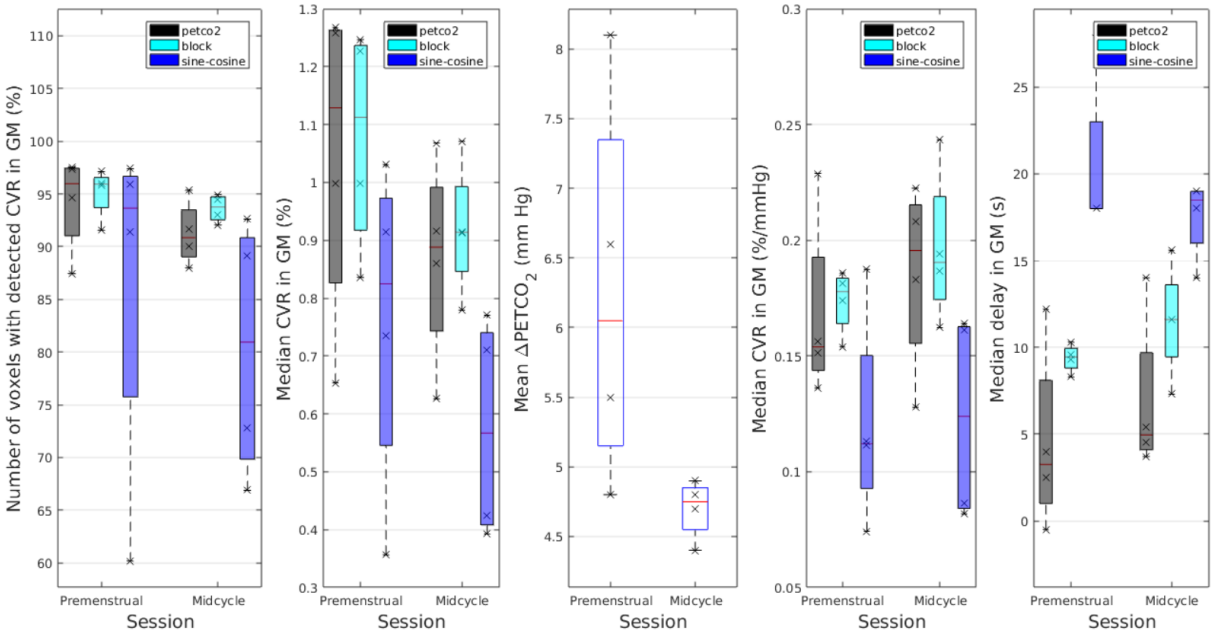

Figure 4: Boxplots representing the distributions of number of voxels with detected CVR, the median CVR in %, mean $\Delta PetCO_2$ in mm Hg and median CVR in %/mm Hg and delays in seconds (from left to right) in GM across controls C2-C5 for both sessions and the 3 analysis methods ($PetCO_2$ in gray, block in cyan and sine-cosine in blue).

hypocapnia and the natural breathing rate calculation might be affected by experimental setup issues.

Using the $PetCO_2$ trace as regressor in the GLM provides a complete model of the hypercapnia stimulus that accounts for inter- and intrasubject variability caused by BH-task performance differences. In addition, it is possible to obtain a quantitative measure of CVR [28]. However, a nasal cannula does not get the expired CO_2 from the mouth that frequently occurs during the task. Thus, a breathing mask seems to be necessary and would probably improve the results obtained using the iteratively shifted $PetCO_2$ GLM analysis method, although it is more uncomfortable and thus can lead to motion. As concerns the sine-cosine GLM method, an analysis should be made assessing the appropriate number of harmonics that better fits the BH BOLD-fMRI considering the task trials duration.

Finally, the number of participants was small (namely patients), which limits the statistical power of the findings and the generalization of the results. Moreover, controlling for the menstrual cycle phase in both groups was done using the calendar method (sometimes together with basal temperature method), which is not completely reliable. Moreover, participants taking hormonal contraception were not excluded, which may have affected cerebrovascular function [20].

References

[1] Laura H. Schulte and Arne May. The migraine generator revisited: Continuous scanning of the migraine cycle over 30 days and three spontaneous attacks. *Brain*, 139(7):1987–1993, 2016.

[2] GBD 2016 Headache Collaborators. Global, regional, and national burden of migraine and tension-type headache, 1990–2016: a systematic analysis for the Global Burden of Disease Study 2016. *The Lancet Neurology*, 17(11):954–976, 2018.

[3] R Pradeep, S. C. Nemichandra, S Harsha, and K Radhika. Migraine Disability, Quality of Life, and Its Predictors. *Annals of Neurosciences*, 27(1):18–23, 2020.

[4] T. J. Steiner, L. J. Stovner, R. Jensen, D. Uluduz, and Z. Katsarava. Migraine remains second among the world's causes of disability, and first among young women: findings from GBD2019. *Journal of Headache and Pain*, 21(1):4–7, 2020.

[5] Andrew Charles. The pathophysiology of migraine: implications for clinical management. *The Lancet Neurology*, 17(2):174–182, 2018.

[6] Kjersti Grøtta Vetvik and E. Anne MacGregor. Menstrual migraine: a distinct disorder needing greater recognition. *The Lancet Neurology*, 20(4):304–315, 2021.

[7] Rami Burstein, Rodrigo Noseda, and David Borsook. Migraine: Multiple processes, complex pathophysiology. *Journal of Neuroscience*, 35(17):6619–6629, 2015.

[8] Peter J. Goadsby, Philip R. Holland, Margarida Martins-Oliveira, Jan Hoffmann, Christoph Schankin, and Simon Akerman. Pathophysiology of migraine: A disorder of sensory processing. *Physiological Reviews*, 97(2):553–622, 2017.

[9] Marina De Tommaso, Anna Ambrosini, Filippo Brighina, Gianluca Coppola, Armando Perrotta, Francesco Pierelli, Giorgio Sandrini, Massimiliano Valeriani, Daniele Marinazzo, Sebastiano Stramaglia, and Jean Schoenen. Altered processing of sensory stimuli in patients with migraine. *Nature Reviews Neurology*, 10(3):144–155, 2014.

[10] Francesca Puledda, Roberta Messina, and Peter J. Goadsby. An update on migraine: current understanding and future directions. *Journal of Neurology*, 264(9):2031–2039, 2017.

[11] David W. Dodick. A Phase-by-Phase Review of Migraine Pathophysiology. *Headache*, 58:4–16, 2018.

[12] Mi Ji Lee, Soohyun Cho, Sook Young Woo, and Chin Sang Chung. Paradoxical association between age and cerebrovascular reactivity in migraine: A cross-sectional study. *Journal of the Neurological Sciences*, 398(September 2018):204–209, 2019.

[13] Swapnil Raut, Upasna Singh, Deepaneeta Sarmah, Aishika Datta, Falguni Baidya, Birva Shah, Mariya Bohra, Priya Jagtap, Ankan Sarkar, Kiran Kalia, Anupom Borah, Kunjan R. Dave, Dileep R. Yavagal, and Pallab Bhattacharya. Migraine and Ischemic Stroke: Deciphering the Bidirectional Pathway. *ACS Chemical Neuroscience*, 11(11):1525–1538, 2020.

[14] Yonghua Zhang, Aasheeta Parikh, and Shuo Qian. Migraine and stroke. *Stroke and Vascular Neurology*, 2(3):160–167, 2017.

[15] Mi Ji Lee, Chungbin Lee, and Chin Sang Chung. The migraine-stroke connection. *Journal of Stroke*, 18(2):146–156, 2016.

[16] Aisha Saeed, Kiran F. Rana, Zain I Warriach, Muhammad Ali Tariq, and Bilal Haider Malik. Association of Migraine and Ischemic Heart Disease: A Review. *Cureus*, 11(9), 2019.

[17] Ahmed N. Mahmoud, Amgad Mentias, Akram Y. Elgendy, Abdul Qazi, Amr F. Barakat, Marwan Saad, Ala Mohsen, Ahmed Abuzaid, Hend Mansoor, Mohammad K. Mojadidi, and Islam Y. Elgendy. Migraine and the risk of cardiovascular and cerebrovascular events: A meta-analysis of 16 cohort studies including 1 152 407 subjects. *BMJ Open*, 8(3):1–10, 2018.

[18] Lise R. Øie, Lise R. Øie, Tobias Kurth, Sasha Gulati, Sasha Gulati, and David W. Dodick. Migraine and risk of stroke. *Journal of Neurology, Neurosurgery and Psychiatry*, 91(6):593–604, 2020.

[19] Dandan Chen, Monica Willis-Parker, and Gina Price Lundberg. Migraine headache: Is it only a neurological disorder? Links between migraine and cardiovascular disorders. *Trends in Cardiovascular Medicine*, 30(7):424–430, 2020.

[20] Jemima S. A. Dzator, Peter R. C. Howe, Lyn R. Griffiths, Kirsten G. Coupland, and Rachel H. X. Wong. Cerebrovascular Function in Hormonal Migraine: An Exploratory Study. *Frontiers in Neurology*, 12(July):1–12, 2021.

[21] Jan Lewis Brandes. The influence of estrogen on migraine: A systematic review. *Journal of the American Medical Association*, 295(15):1824–1830, 2006.

[22] Garrett L. Peltonen, John W. Harrell, Benjamin P. Aleckson, Kaylie M. LaPlante, Meghan K. Crain, and William G. Schrage. Cerebral blood flow regulation in women across menstrual phase: Differential contribution of cyclooxygenase to basal, hypoxic, and hypercapnic vascular tone. *American Journal of Physiology - Regulatory Integrative and Comparative Physiology*, 311(2):R222–R231, 2016.

[23] Anne H. Calhoun. Understanding Menstrual Migraine. *Headache*, 58(4):626–630, 2018.

[24] Jemima S.A. Dzator, Peter R.C. Howe, and Rachel H.X. Wong. Profiling cerebrovascular function in migraine: A systematic review and meta-analysis. *Journal of Cerebral Blood Flow and Metabolism*, 2020.

[25] Suk Tak Chan, Karleyton C. Evans, Tian Yue Song, Rajiv Gupta, Bruce R. Rosen, Aneesh Singhal, and Kenneth K. Kwong. Functional magnetic resonance imaging of regional impaired cerebrovascular reactivity for migraineurs in the interictal state. *bioRxiv*, 7194(617), 2019.

[26] Silva Cotrim, R Gil-Gouveia, J Pinto, P Vilela, Martins I Pavão, and P Figueiredo. Increased cerebrovascular reactivity during spontaneous migraine attacks compared to pain-free periods. *Proc. 37th Annual Scientific Meeting of the European Society for Magnetic Resonance in Medicine and Biology (ESMRMB 2020)*, 2020.

[27] Ilona Lipp, Kevin Murphy, Xavier Caseras, and Richard G. Wise. Agreement and repeatability of vascular reactivity estimates based on a breath-hold task and a resting state scan. *NeuroImage*, 113:387–396, 2015.

[28] Joana Pinto, Molly G. Bright, Daniel P. Bulte, and Patrícia Figueiredo. Cerebrovascular Reactivity Mapping Without Gas Challenges: A Methodological Guide. *Frontiers in Physiology*, 11:320–326, 2021.

[29] Molly G. Bright and Kevin Murphy. Reliable quantification of BOLD fMRI cerebrovascular reactivity despite poor breath-hold performance. *NeuroImage*, 83:559–568, 2013.

[30] Adam L. Urback, Bradley J. MacIntosh, and Benjamin I. Goldstein. Cerebrovascular reactivity measured by functional magnetic resonance imaging during breath-hold challenge: A systematic review. *Neuroscience and Biobehavioral Reviews*, 79:27–47, 2017.

[31] Arne May. Understanding migraine as a cycling brain syndrome: reviewing the evidence from functional imaging. *Neurological Sciences*, 38:125–130, 2017.

[32] Simona Sacco, Silvia Ricci, Diana Degan, and Antonio Carolei. Migraine in women: The role of hormones and their impact on vascular diseases. *Journal of Headache and Pain*, 13(3):177–189, 2012.

[33] Jes Olesen. Headache Classification Committee of the International Headache Society (IHS) The International Classification of Headache Disorders, 3rd edition. *Cephalalgia*, 38(1):1–211, 2018.

[34] S. Tasdemir, H. Akgun, S. Mazman, E. Eroglu, S. Alay, M. Yucel, O. Oz, U. Ulas, and S. Demirkaya. Evaluation of Cerebral Hemodynamics of Patients with Menstrual Migraine. *Cephalgia*, 33(8):166, 2013.

[35] Roopa Rajan, Dheeraj Khurana, and Vivek Lal. Interictal cerebral and systemic endothelial dysfunction in patients with migraine: A case-control study. *Journal of Neurology, Neurosurgery and Psychiatry*, 86(11):1253–1257, 2014.

[36] D. Perko, J. Pretnar-Oblak, M. Šabovič, B. Žvan, and M. Zaletel. Cerebrovascular reactivity to l-arginine in the anterior and posterior cerebral circulation in migraine patients. *Acta Neurologica Scandinavica*, 124(4):269–274, 2011.

[37] Mauro Silvestrini, Letizia M. Cupini, Elio Troisi, Maria Matteis, and Giorgio Bernardi. Estimation of cerebrovascular reactivity in migraine without aura. *Stroke*, 26(1):81–83, 1995.

[38] Fumihiko Sakai and John Stirling Meyer. Abnormal Cerebrovascular Reactivity in Patients with Migraine and Cluster Headache. *Headache: The Journal of Head and Face Pain*, 19(5):257–266, 1979.

[39] C Harer and R Kummer. Cerebrovascular CO_2 reactivity in migraine: assessment by transcranial Doppler ultrasound. *Journal of Neurology*, 238:23–26, 1991.

[40] Raffaele Ornello, Ilaria Frattale, Valeria Caponnetto, Francesca Pistoia, and Simona Sacco. Cerebral vascular reactivity and the migraine-stroke relationship: A narrative review. *Journal of the Neurological Sciences*, 414(May), 2020.

[41] J. Krejza, W. Rudzinski, M. Arkuszewski, O. Onuoha, and E. R. Melhem. Cerebrovascular reactivity across the menstrual cycle in young healthy women. *Neuroradiology Journal*, 26(4):413–419, 2013.

[42] Kevin Murphy, Ashley D. Harris, and Richard G. Wise. Robustly measuring vascular reactivity differences with breath-hold: Normalising stimulus-evoked and resting state BOLD fMRI data. *NeuroImage*, 54(1):369–379, 2011.

[43] Stefano Moia, Rachael C. Stickland, Apoorva Ayyagari, Maite Termenon, Cesar Caballero-Gaudes, and Molly G. Bright. Voxelwise optimization of hemodynamic lags to improve regional CVR estimates in breath-hold fMRI. *Proceedings of the Annual International Conference of the IEEE Engineering in Medicine and Biology Society, EMBS*, 2020-July:1489–1492, 2020.

[44] Richard B Buxton. Introduction to Functional Magnetic Resonance Imaging: Principles and Techniques. *Cambridge University Press*, 2009.

[45] Andreas Kastrup, Tie-qiang Li, Atsuchi Takahashi, Gary H Glover, and Michael E Moseley. Short Communications Cerebral Blood Oxygenation Changes. pages 2641–2645, 1998.

[46] F. H. Van der Zande, P. A. Hofman, and W. H. Backes. Mapping hypercapnia-induced cerebrovascular reactivity using BOLD MRI. *Neuroradiology*, 47(2):114–120, 2005.

[47] Rachael C. Stickland, Kristina M. Zvolanek, Stefano Moia, Apoorva Ayyagari, César Caballero-Gaudes, and Molly G. Bright. A practical modification to a resting state fMRI protocol for improved characterization of cerebrovascular function. *NeuroImage*, 239, 2021.

[48] Joana Pinto, João Jorge, Inês Sousa, Pedro Vilela, and Patrícia Figueiredo. Fourier modeling of the BOLD response to a breath-hold task: Optimization and reproducibility. *NeuroImage*, 135:223–231, 2016.

[49] Molly G. Bright, Manus J. Donahue, Jeff H. Duyn, Peter Jezzard, and Daniel P. Bulte. The effect of basal vasodilation on hypercapnic and hypocapnic reactivity measured using magnetic resonance imaging. *Journal of Cerebral Blood Flow and Metabolism*, 31(2):426–438, 2011.

[50] S. D. Goode, S. Krishan, C. Alexakis, R. Mahajan, and D. P. Auer. Precision of cerebrovascular reactivity assessment with use of different quantification methods for hypercapnia functional MR imaging. *American Journal of Neuroradiology*, 30(5):972–977, 2009.

[51] Felipe B. Tancredi and Richard D. Hoge. Comparison of cerebral vascular reactivity measures obtained using breath-holding and CO 2 inhalation. *Journal of Cerebral Blood Flow and Metabolism*, 33(7):1066–1074, 2013.

[52] Sridhar S. Kannurpatti, Michael A. Motes, Bart Rypma, and Bharat B. Biswal. Increasing measurement accuracy of age-related BOLD signal change: Minimizing vascular contributions by resting-state-fluctuation-of-amplitude scaling. *Human Brain Mapping*, 32(7):1125–1140, 2011.

[53] Alex A. Bhogal, Jeroen C.W. Siero, Joseph A. Fisher, Martijn Froeling, Peter Luijten, Marielle Philippens, and Hans Hoogduin. Investigating the non-linearity of the BOLD cerebrovascular reactivity response to targeted hypo/hypercapnia at 7T. *NeuroImage*, 98:296–305, 2014.

[54] Fatemeh Geranmayeh, Richard J.S. Wise, Robert Leech, and Kevin Murphy. Measuring vascular reactivity with breath-holds after stroke: A method to aid interpretation of group-level BOLD signal changes in longitudinal fMRI studies. *Human Brain Mapping*, 36(5):1755–1771, 2015.